PNC TN9410 96-102

Thermal Fluid-Structure Interaction Analysis of Shield Plug (Ⅱ)

—Verification of FLUSH by Two-Dimensional Model—

April 1996

Power Reactor and Nuclear Fuel Development Corporation

O-arai Engineering Center

Technology Management Section
O-arai Engineering Center
Power Reactor and Nuclear Fuel Development Corporation
4002 Narita-machi, O-arai-machi, Higashi-Ibaraki, Ibaraki-Ken, 311-13

Ⓝ

公　開　資　料
PNC TN9410 96-102
1 9 9 6 年 4 月

熱流体-構造連成解析による遮蔽プラグ解析（II）

- 2次元モデルによるFLUSHの検証 -

宋　小明＊、大平　博昭＊＊

要　旨

高速炉の炉上部構造におけるカバーガス領域の熱流力特性と遮蔽プラグの温度特性とを連成させて解析する熱流体-構造連成解析コード（FLUSH）を、大洗工学センターで過去に実施した実験結果を用いて検証した。

解析では、ナトリウム液面を模擬したアルミニウムの高温面からの輻射伝熱をも考慮し、カバーガスの自然対流による熱流力特性と回転プラグを模擬した構造物の温度場とを２次元体系でモデル化し、実験で行われたナトリウムミストを含まない８ケースの条件とした。

解析の結果、８ケースの実験条件に対して、カバーガス領域の流速及び温度分布と模擬回転プラグ内の半径方向及び軸方向の温度分布の両者が熱的に連続した状態で得られた。また、本８ケースではカバーガス領域と模擬回転プラグ間の境界温度は同傾向であり、境界温度の平均値は実験結果と1.3%以下の差で一致した。さらに構造物内の温度分布は、ガバーガス自然対流による影響が支配的であり、輻射伝熱の効果は比較的小さくアルミニウム板の温度が400℃以下であれば無視できることがわかった。

＊　原子力交流制度に基づく研修生。大洗工学センター基盤技術開発部熱流体技術開発室（在籍期間：1995年10月8日～1996年3月29日）において研修。（現：中国核動力研究設計院）

＊＊ 大洗工学センター　基盤技術開発部　熱流体技術開発室

PNC TN9410 96-102
April, 1996

Thermal Fluid-Structure Interaction Analysis of Shield Plug (II)

- Verification of FLUSH by Two-Dimensional Model -

Xiaoming Song*
Hiroaki Ohira**

ABSTRACT

In designing the shield plug of LMFBR, it is important to evaluate the thermal response between the cover gas thermal-hydraulics and the temperature fields of the shield plug at the same time. Based on the experiments which were performed by OEC, the natural convection and the thermal radiation in the cover gas layer were calculated with the structure simulating the shield plug in a detail two-dimensional model. The calculations were carried out for 8 kinds of experimental RUNs using a FLUSH code.
The main results were as follows:

- For these 8 kinds of experimental RUNs, the velocity and the temperature distributions in the cover gas layer were presented. The radial and axial temperature distributions in the rotating plug were also presented, which were difficult to measure by the experiments.

- The boundary surface temperature between the cover gas layer and the rotating plug had the same tendencies and the calculated average temperatures on the boundary surface had good agreements with the experimental data. The average relative deviations from experimental values were less than 1.3%.

- The natural convection of the cover gas enhanced the temperature distributions in the structure. The effects of thermal radiation on the heat transfer was relatively small and it can be neglected when the temperature of the heated aluminum disk is less than 400°C.

---

* Assignee of the Scientist Exchange Program in Nuclear Energy Research between Japan and Neighbouring Countries from October 8, 1995 to March 29, 1996 at Thermal-Hydraulic Research Section, O-arai Engineering Center, PNC.
(Present organization: Nuclear Power Institute of China, P.R.China)

** Thermal-Hydraulic Research Section, O-arai Engineering Center, PNC, Japan

CONTENTS

LIST OF TABLES

LIST OF FIGURES

NOMENCLATURES

A_{Al} : Area of surface of heated aluminum disk
A_{UG} : Area of lower surface of rotating plug
C_0 : Constant of properties
C_1 : Constant of properties
C_p : Specific heat
Dev : Average relative deviation from the experimental value
F : Shape factor
H : Heat transfer coefficient
h : Enthalpy
I,J,K : Cell or Element indices in the r-, θ-, and z-directions
k : Thermal conductivity
l : The distance from the cell center to the boundary
N : The number of nodes on boundary surface
Q : Heat
q : Heat flux
r : Radial coordinate
T_{Al} : Temperature of heated aluminum disk
T_{UG} : Temperature of rotating plug lower surface
T_{av} : Calculated average boundary surface temperature
T_{exp} : Experimental average boundary surface temperature
T_i : Temperature of node i on boundary surface
$\overline{T}$: The average temperature in the cover gas layer
z : Axial coordinate
α : Relaxation factor
ε_{Al} : Emmisivity of heated aluminum disk surface
ε_{UG} : Emmisivity of rotating plug surface
ρ : Density
σ : Radiant constant
θ : Circumference coordinate
μ : Viscosity
g : Gravitational acceleration
β : Volume expansion coefficients
Gr : Gr number
Pr : Pr number
Ra : Ra number

1. INTRODUCTION

In designing the shield plug of LMFBR, the heat transfer characteristics from liquid sodium surface to the shield plug through cover gas layer is important to evaluate the thermal stress of the structure and the performance of the cooling system. In June 1979, a series of tests on heat transfer to the rotating plug through the cover gas layer were conducted in OEC [1]. Detail experiments were carried out regarding the natural convection in the cover gas layer and the thermal radiation heat transfer between the heated aluminum disk and the rotating plug.

The objective of this work is to verify a FLUSH code for simulating the heat transfer to rotating plug through the cover gas layer in an LMFBR reactor vessel. In addition the following information is provided:

- The accuracy of FLUSH for the analysis of the heat transfer between fluid and structure.
- The effects of the temperature distributions in the structure, especially, on the boundary surface temperatures which were resulted from the cover gas natural convection and the thermal radiation.
- The acquisition of a lot of calculated results which are difficult to measure in the experiments, for instance, the velocity vector and the temperature distributions in the cover gas layer, and the temperature distributions in the rotating plug.

In order to evaluate these effects, detailed two-dimensional models including the cover gas layer and the rotating plug were created. Based on the experimental results, the calculations of the heat transfer to the rotating plug through the cover gas layer were carried out for 8 kinds of experimental RUNs. The calculated results were compared with the experimental results.

2. EXPERIMENTAL APPARATUS

Figure 2.1 shows a schematic of a test vessel. The main components consist of the heated aluminum disk which can be moved in the vertical direction, and the heat flux measuring section which simulates the rotating plug in an LMFBR. A 300-millimetre-thick thermal insulator surrounds the outside wall of the test vessel and an auxiliary heater in the center of the thermal insulator is installed so that the thermal loss in the radial direction to be compensated. In the inside wall of the test vessel, a circular radiation shield is arranged in order to reduce the thermal loss in the radial direction as little as possible. Argon (Ar) gas and Helium (He) gas were used as the cover gas in this experiment.

Figure 2.2 shows the circular heated aluminum disk. It is heated by the heater. In order to reduce the radiant heat transfer from the heated aluminum disk to the heat flux measuring section, a 5-millimetre-thick commercial aluminum plate was installed on the upper surface of the aluminum disk. Several thermocouples were arranged for the temperature measurement of the heated aluminum disk. The heated aluminum disk can be moved in the vertical direction so that the thickness of the cover gas layer can be changed from 100 to 300 millimetres. In this experiment, the thickness of the cover gas layer was set at the constant level of 100 millimeters.

Figure 2.3 shows the heat flux measuring section which was made by circular stainless plate (SUS-304). The thickness of the heat flux measuring section was 40 millimetres and the upper surface was covered with 5-millimetre-thick Helium gas. Several thermocouples were arranged on the lower and upper surfaces of the heat flux measuring section, and they were also arranged in the Helium gas layer.

3. FLUSH CODE

The calculations were performed using a FLUSH code which include two computer programs called AQUA and FINAS.

AQUA is a new version of COMMIX-1A computer program[2] which was developed by Argonne National Laboratory (ANL) under sponsorship of the U.S. Nuclear Regulatory Commission (USNRC). COMMIX-1A is a general-purpose thermal-hydraulic code that can be used to calculate multi-dimensional steady/unsteady reactor component fluid-flow problems. The general background and equations solved by COMMIX-1A have been reported in reference [2]. This code has been released from ANL to PNC through the USNRC in January, 1983. After the code was released to PNC, much modification was carried out by PNC/OEC and the modified code was named an AQUA code which was used extensively in PNC. The input manual for the use of the code has been documented in the PNC report in Japanese[3].

FINAS (Finite Element Nonlinear Structure Analysis System) has been developed by PNC/OEC which can be used to analyze multi-dimensional steady/unsteady reactor structure component thermal-stress and heat transfer problems. The input manual for the use of the code has been documented in the PNC report in Japanese[4]. In this calculation, FINAS code was used to analyze the temperature fields in the rotating plug.

The FLUSH code[5] can be used to calculate the heat transfer problems between fluid and structure through AQUA and FINAS. Using the two results, the temperature distribution on boundary surface between fluid and structure can be determined by iterative calculations.

4. MODELING

4.1 Geometry

The geometrical details have been taken from the reference[1]. Figure 2.1 shows the detailed geometrical model (experimental vessel). Considering the symmetry of the experimental vessel in the azimuthal direction, the two-dimensional model can be used. In this calculation, efforts were made to create a numerical model in detail to avoid extremely long computer-time.

Figure 4.1 shows the simple geometrical model which is only 1/36-sector of the cover gas layer and the heat flux measuring section (rotating plug) in the experimental vessel. The radial length of the cover gas layer is 282.5 millimetres, and the height of 100 millimetres. Ar gas was used as the cover gas. The heat flux measuring section (rotating plug) is made of stainless steel (SUS304). The radial length of heat flux measuring section is the same as that of the cover gas layer, and the height of 40 millimetres.

4.2 Mesh Arrangement

Figure 4.2 shows the mesh arrangement for the two-dimensional model which is divided into two parts; the cover gas layer and the structure region simulating the rotating plug (heat flux measuring section).

4.2.1 Cover Gas Layer

- Coordinate system : Cylindrical coordinate
- I-Direction (radial direction) : Divided into 29 sections
- J-Direction (circumference direction) : 1 section
- K-Direction (axial direction) : Divided into18 sections
- Number of cells : 522
- Number of surfaces : 1138
- Number of boundary surfaces : 6

4.2.2 Rotating Plug (Heat Flux Measuring Section)

- Coordinate system : Cylindrical coordinate
- I-Direction (radial direction) : Divided into 25 sections
- J-Direction (circumference direction) : 1 section
- K-Direction (axial direction) : Divided into 8 sections

- Number of nodes : 468
- Number of elements : 200

4.3 Analysis Conditions

4.3.1 Properties

In this calculation, the properties of Ar gas such as enthalpy, density, thermal conductivity and viscosity were all assumed to be the linear functions of only temperature:

$$h = C_{0h} + C_{1h}\,T, \quad C_{0h} = 1.43216\times10^{5}, \quad C_{1h} = 5.21\times10^{2} \tag{4-1}$$

$$\rho = C_{0\rho} + C_{1\rho}\,T, \quad C_{0\rho} = 2.338851, \quad C_{1\rho} = -2.978776\times10^{-3} \tag{4-2}$$

$$k = C_{0k} + C_{1k}\,T, \quad C_{0k} = 1.7181110^{-2}, \quad C_{1k} = 3.9417110^{-5} \tag{4-3}$$

and

$$m = C_{0m} + C_{1m}\,T, \quad C_{0m} = 2.2333610^{-5}, \quad C_{1m} = 4.9028610^{-8} \tag{4-4}$$

Where, Co and C_1 are the constants, and they were input as the NAMELIST formats in AQUA.

The properties of SUS304 such as thermal conductivity, specific heat capacity and density were input as the table formats in FINAS. Table 4-1 shows these properties.

4.3.2 Boundary Conditions

The boundary conditions which were used in this calculation are listed in table 4-2. They are decided from the experimental results.

4.3.3 Heat Transfer Coefficient

In order to reduce the deviation deduced from the simplification of heat transfer correlation, the heat transfer from the cover gas to the rotating plug was modeled by using the small size mesh (about 1 millimetre) near the boundary surface. The heat transfer coefficients on the each boundary cell surface; H, can be evaluated as follows:

$$H = k/l \tag{4-5}$$

where,

k : thermal conductivity of Ar gas,

l : the distance from the cell center to the boundary.

4.3.4 Turbulence Model

In this calculation, the turbulent model was not used.

4.3.5 Force Structure Model

In this calculation, the force structure model was not used.

4.3.6 Heat Conduction

HHEX8 model which is a cube of six surfaces was used as the heat conduction model.

4.3.7 Thermal Radiation

The transferred heat quantity by radiation between the heated aluminum disk and the surface of rotating plug (the heat flux measuring section) can be evaluated according to following formulas:

$$Q = \frac{\sigma(T_{Al}^4 - T_{UG}^4)}{\frac{1-\varepsilon_{Al}}{\varepsilon_{Al}A_{Al}} + \frac{1}{A_{Al}F} + \frac{1-\varepsilon_{UG}}{\varepsilon_{UG}A_{UG}}} \qquad (4\text{-}6)$$

where,

Q : the amount of heat by the thermal radiation,
ε_{Al} : the emmisivity of heated aluminum disk,
ε_{UG} : the emmisivity of rotating plug surface,
A_{Al} : the area of surface of the heated aluminum disk,
A_{UG} : the area of the lower surface of the rotating plug,
σ : the radiant constant,
F : the shape factor, its value is related to the relative position of emitted surfaces,
T_{Al} : the temperature of the heated aluminum disk,
T_{UG}: the temperature of the rotating plug lower surface.

According to the experimental results, the following emissivities were used:

$$\varepsilon_{Al} = 0.09 \qquad (4\text{-}7)$$

$$\varepsilon_{UG} = 0.16 \qquad (4\text{-}8)$$

The shape factor F was calculated in detail using the formula in the reference[6].

4.3.8 FLUSH Iteration

The method of heat flux iteration used in FLUSH is as follows:

$$q^{n+1}{}_{new} = (q^{n+1} - q^n) \alpha + q^n , \qquad \alpha = 0.5 \qquad (4\text{-}9)$$

The convergence criteria of temperature iteration is as follows:

$$\max\left|\frac{T_j^{i+1}-T_j^i}{T_j}\right| \leq 3.0\times10^{-4} \qquad (4\text{-}10)$$

5. RESULTS AND DISCUSSIONS

5.1 Results

The calculated results for eight kinds of experimental RUNs are described bellow regarding the natural convection in the cover gas layer, the temperature distributions in the cover gas layer, the temperature distributions in the rotating plug, and the radial temperature distributions on the boundary surface.

5.1.l Natural Convection in Cover Gas Layer

Because of the temperature difference in the cover gas layer, there must deduce the natural convection in the cover gas layer. Figure 5.1.1 shows the distribution of calculated velocity vectors in the cover gas layer for eight kinds of experimental RUNs. By comparing these figures, it is found that the distributions of eight kinds of experimental RUNs almost have the same flow pattern. The characteristics of the calculated flow pattern were as follows:

- Clock-wise natural circulation was formed in the cover gas layer,

- The velocity vectors near the walls were larger than these in the other area since the temperature differences near the wall were larger. The largest velocity vector in the cover gas layer was about 0.5 m/sec.

5.1.2 Temperature Distribution in Cover Gas Layer

The temperature distributions in the cover gas layer for eight kinds of experimental RUNs are shown in the form of isothermal line in Figure 5.1.2. From these figures, it is clear that the pattern of the temperature distributions in the cover gas layer of eight kinds of experimental RUNs have quite similar tendencies. They show the typical temperature distributions of natural convection.

5.1.3 Temperature Distribution in Rotating Plug

The temperature distributions in the rotating plug for eight kinds of experiments are shown in Figs 5.1.3 and 5.1.4. Figure 5.1.3 shows the radial temperature distributions at different axial positions and Figure 5.1.4 shows the axial temperature distributions at different radial positions. Comparing these figures, the same conclusion can be deduced that the temperature distributions in the rotating plug had the same tendencies. The highest temperature appeared in the center of the lower surface of the rotating plug and the lowest temperature on the upper surface of the rotating plug.

5.1.4 Boundary Surface Temperature Distribution Between Cover Gas Layer and Rotating Plug

The boundary temperature distributions between the cover gas layer and the rotating plug for eight kinds of experimental RUNs are also shown in Figure 5.1.3. Naturally, as analyzed above, temperature distributions on the boundary surface between the cover gas layer and the rotating plug were the same. The highest temperature was in the circle center of the boundary surface, and then, it gradually becomes lower in the radial direction until the lowest temperature in the circumference of the boundary surface.

Table 5-1 shows the measured average temperatures and the calculated ones on the boundary surface. T_{av} and Dev in the table are defined as follow:

$$T_{av} = \frac{1}{N} \sum_{i=1}^{N} T_i \tag{5-1}$$

$$D_{ev} = \left| \frac{T_{av} - T_{exp}}{T_{exp}} \right| \times 100\ (\%) \tag{5-2}$$

where,

Tav	: Calculated average temperature on the boundary surface,
T_i	: Temperature of the mesh node i on the boundary surface,
N	: Total number of the node on the boundary surface,
T_{exp}	: Experimental average temperature on the boundary surface,
Dev	: Average relative deviation from the experimental dates.

It can be seen that the average relative deviation from the experimental results for each experimental RUN is less than 1.3%.

5.2 Discussions

The heat transfer by the thermal radiation between the heated aluminum disk and the rotating plug was not simulated in the above calculation. In fact, the thermal radiation heat transfer exists from the heated aluminum disk to the rotating plug, because of the temperature difference. Especially, the effects are expected to be larger on the condition of higher temperature on the heated aluminum disk. Therefore, the effects of aluminum temperature must be studied. In order to do this, several experimental RUNs were studied which had higher temperatures on the heated aluminum disk based on the following 3 cases:

- Case-1: The thermal radiation heat transfer (RTH) between the heated aluminum disk and the rotating plug was calculated and the natural convection (NC) in cover gas layer was neglected. (with RHT)

- Case- 2: The natural convection in the cover gas layer was also calculated. (without RHT)

- Case- 3: Both thermal radiation and natural convection were calculated. (with NC and RHT)

Figure 5.2.1 shows the calculated velocity vectors in the cover gas layer, the calculated isotherms in the cover gas layer and the radial temperature distributions in the rotating plug on the condition of Case-3 of the experimental RUN 6. The highest temperature was measured on this condition. Figure 5.2.2 shows the temperature distributions on the boundary surface of 3 cases, and Table 5-2 shows the average temperatures on the boundaries in Case-2 and -3. These include the results of Case-2 which were also shown in Section 5.1. Comparing Case-2 with Case-3, it is found that the velocity vectors, the temperature distributions in cover gas layer and the radial temperature distributions in rotating plug have the same tendencies between the two cases. From these results, the following information can be deduced:

- On the condition of Case-1, the boundary surface temperature in the radial direction had small distribution. The maximum temperature difference was about 2°C. The calculated average temperature on the boundary surface was smaller than the experimental values.

- On the condition of Case-2, the temperature difference on the boundary surface in radial direction was large and the maximum temperature difference was about 10°C. Thus, the natural convection in the cover gas layer enhanced the temperature difference in the rotating plug. The calculated average boundary temperature agreed well with the experimental values in the experimental RUNs and the average relative deviations from the experimental values was less than 1.3%.

- On the condition of Case-3, the temperature distributions on the boundary surface had the similar tendencies to those in Case-2. The only difference was that the boundary surface temperature in Case-3 was higher than that in Case-2. However, the average boundary surface temperature was nearly equal at both cases. From Table 5-2, it can be seen that the difference of average temperature of both cases was less than 1.3 °C. Therefore, it can be concluded that the effects of thermal radiation heat transfer were very small and it does not make large deviations on calculated results if it is neglected. Especially at the

case of experimental RUNs 7 through 10, the thermal radiation heat transfer can be neglected since the temperature of heated aluminum disk are very low.

In Section 5.1.1, it was concluded that the velocity distributions in the cover gas layer at eight kinds of experimental RUNs almost have the same pattern. This can be discussed as follows:

At the condition of natural convection, the Raylay number can be calculated using following definitions:

$$Ra = GrPr \tag{5-3}$$

$$Gr = \frac{g\beta\rho^3 L^3(\overline{T} - T_{U.G})}{\mu^3} \tag{5-4}$$

$$\overline{T} = T_{Al} - T_{U.G} \tag{5-5}$$

$$Pr = \frac{C_p\mu}{k} \tag{5-6}$$

Where,

Ra	: Ra number,
Gr	: Gr number,
Pr	: Pr number,
$\overline{T}$	: The average temperature in the cover gas layer,
C_p	: specific heat capacity,
k	: thermal conductivity,
T_{Al}	: emperature of heated aluminum disk,
T_{UG}	: temperature of rotating plug lower surface,
ρ	: density,
μ	: viscosity,
L	: defined length,
g	: gravitational acceleration,
β	: volume expansion coefficients.

If the radial length of cover gas layer was used as the defined length of the formulas, the Raylay numbers of the experimental RUNs were about $4.4\text{-}7.9 \times 10^7$. They were almost the same order. That is the reason why the velocity distributions in the cover gas layer at the experimental RUNs almost have the same pattern.

6. CONCLUSIONS

The detailed two-dimensional analysis of heat transfer to the rotating plug through the cover gas layer for 8 kinds of experimental RUNs were performed by using FLUSH. The main conclusions were as follows:

- For these 8 kinds of experimental RUNs, the velocity and the temperature distributions in the cover gas layer were presented. The radial and axial temperature distributions in the rotating plug were also presented, which were difficult to measure by the experiments.

- The boundary surface temperature between the cover gas layer and the rotating plug had the same tendencies and the calculated average temperature on the boundary surface had good agreements with the experimental values. The average relative deviations from experimental values were less than 1.3%.

- The natural convection of the cover gas enhanced the temperature distributions in the structure. The effects of thermal radiation to the heat transfer was relatively small and it can be neglected when the temperature of the heated aluminum disk is less than 400°C.

ACKNOWLEDGMENT

Many thanks to Mr. T. Iwasaki and Mr. H. Yonekawa, the members of Grope 3, Nuclear Energy System Inc. Ltd. for their help and many useful suggestions in our work.

REFERENCES

[1] O. Furukawa, et al., " Heat Transfer to Rotating Plug Through Cover Gas in LMFBR Reactor Vessel ", Proc. of 19th National Heat Transfer Symposium of Japan, May 1982

[2] H. M. Domanus, et al., " COMMIX-1A: A Three-Dimensional Transient Single-Phase Computer Program for Thermal Hydraulic Analysis of Single and Multi-component System ", ANL Draft Report, September 1982

[3] T. Muramatsu, et al., PNC Technical Review, PNC TN9520 90-004 (in Japanese), 1990

[4] Kouji Iwata, " Finite Element Nonlinear Structure Analysis System ", PNC TN9520 92-006, Version 12.0 (in Japanese), March 1993

[5] H. Ohira, " Interface Program for the Interaction between Thermal-hydraulics and Thermal Structure Response ", PNC TN1340 89-003, September 1989

[6] H. Ohira, " Thermal Fluid-Structure Interaction Analysis for the Upper Structure of FBR ", PNC TN9410 96-148 (in Japanese), 1996

Table 4-1 Properties of SUS304

Temperature (℃)	Conductivity (kcal/mm.s.℃)	Heat Capacity (kcal/kg.℃)	Density (Kg/mm^3)
20	3.48E-06	0.108	8.03E-06
50	3.53E-06	0.112	8.02E-06
100	3.73E-06	0.118	8.00E-06
150	3.89E-06	0.122	7.97E-06
200	4.05E-06	0.125	7.95E-06
250	4.21E-06	0.128	7.93E-06
300	4.37E-06	0.129	7.90E-06
350	4.53E-06	0.131	7.88E-06
400	4.70E-06	0.132	7.86E-06
450	4.86E-06	0.133	7.83E-06
500	5.02E-06	0.134	7.81E-06
550	5.18E-06	0.136	7.79E-06
600	5.34E-06	0.138	7.76E-06
650	5.51E-06	0.14	7.74E-06
700	5.67E-06	0.142	7.72E-06
750	5.83E-06	0.145	7.70E-06
800	5.89E-06	0.147	7.67E-06

Table 4-2 Boundary Conditions

Run number	The aluminum plate surface* (℃)	The upper surface of the structure* (℃)
1	363.1	160.2
2	404.3	180.9
3	407.0	182.8
6	410.5	186.4
7	337.2	153.4
8	292.7	131.1
9	290.9	129.1
10	235.8	102.3

* The experimental average temperature from reference 1

Table 5-1 The Calculated Boundary Temperatures

Radial location (mm)	Temperature on the boundary (°C)							
	RUN 1	RUN 2	RUN 3	RUN 6	RUN 7	RUN 8	RUN 9	RUN 10
0.0	169.16	190.86	190.88	194.48	159.67	136.39	134.41	106.44
11.3	168.67	190.32	190.64	194.25	159.49	136.24	134.25	106.32
22.6	168.03	189.62	190.28	193.89	159.21	136.01	134.01	106.13
33.9	167.43	188.95	189.88	193.48	158.90	135.74	133.74	105.92
45.2	166.86	188.32	189.46	193.07	158.58	135.48	133.47	105.71
56.5	166.34	187.85	189.06	192.66	158.26	135.21	133.21	105.51
67.8	165.86	187.23	188.67	192.27	157.96	134.96	132.95	105.31
79.1	165.43	186.75	188.31	191.91	157.68	134.71	132.71	105.12
90.4	165.04	186.32	187.97	191.56	157.41	134.49	132.48	104.94
101.7	164.69	185.94	187.65	191.25	157.17	134.28	132.27	104.78
113.0	164.38	185.59	187.35	190.95	156.93	134.08	132.08	104.63
124.3	164.09	185.27	187.08	190.68	156.72	133.90	131.90	104.49
135.6	163.83	184.98	186.83	190.43	156.52	133.74	131.73	104.36
146.9	163.60	184.75	186.60	190.19	156.34	133.58	131.58	104.24
158.2	163.39	184.50	186.39	189.98	156.18	133.44	131.44	104.13
169.5	163.21	184.29	186.39	189.79	156.03	133.32	131.31	104.03
180.8	163.04	184.10	186.02	189.61	155.89	133.20	131.19	103.94
192.1	162.88	183.92	185.85	189.44	155.76	133.09	131.08	103.85
203.4	162.74	183.76	185.69	189.29	155.63	132.98	130.98	103.77
214.7	162.60	183.61	185.54	189.14	155.52	132.89	130.88	103.69
226.0	162.47	183.47	185.40	189.00	155.41	132.80	130.79	103.62
237.3	162.34	183.32	185.27	188.86	155.30	132.71	130.70	103.55
248.6	162.22	183.18	185.14	188.73	155.20	132.62	130.62	103.48
259.9	162.10	183.06	185.02	188.61	155.11	132.54	130.54	103.42
271.2	161.99	182.94	184.92	188.51	155.04	132.48	130.47	103.37
282.5	161.94	182.88	184.87	188.47	155.00	132.47	130.44	103.35
Tav	164.40	185.60	187.20	190.79	156.80	133.97	131.95	104.52
Texp	162.30	183.40	185.30	188.90	155.30	132.90	130.90	103.70
Dev	1.29%	1.20%	1.03%	1.00%	0.97%	0.81%	0.80%	0.79%

Table 5-2 The Calculated Boundary Temperature with/without Radiation

Run number	with NC and RHT (Case-3)		without RHT (Case-2)		Experiment
	Average Temperature	Average Deviation	Average Temperature	Average Deviation	Average Temperature
	(°C)	(%)	(°C)	(%)	(°C)
1	165.1	1.73	164.4	1.29	162.3
2	186.6	1.74	185.6	1.20	183.4
3	188.6	1.76	187.2	1.03	185.3
6	192.1	1.70	190.8	1.00	188.9

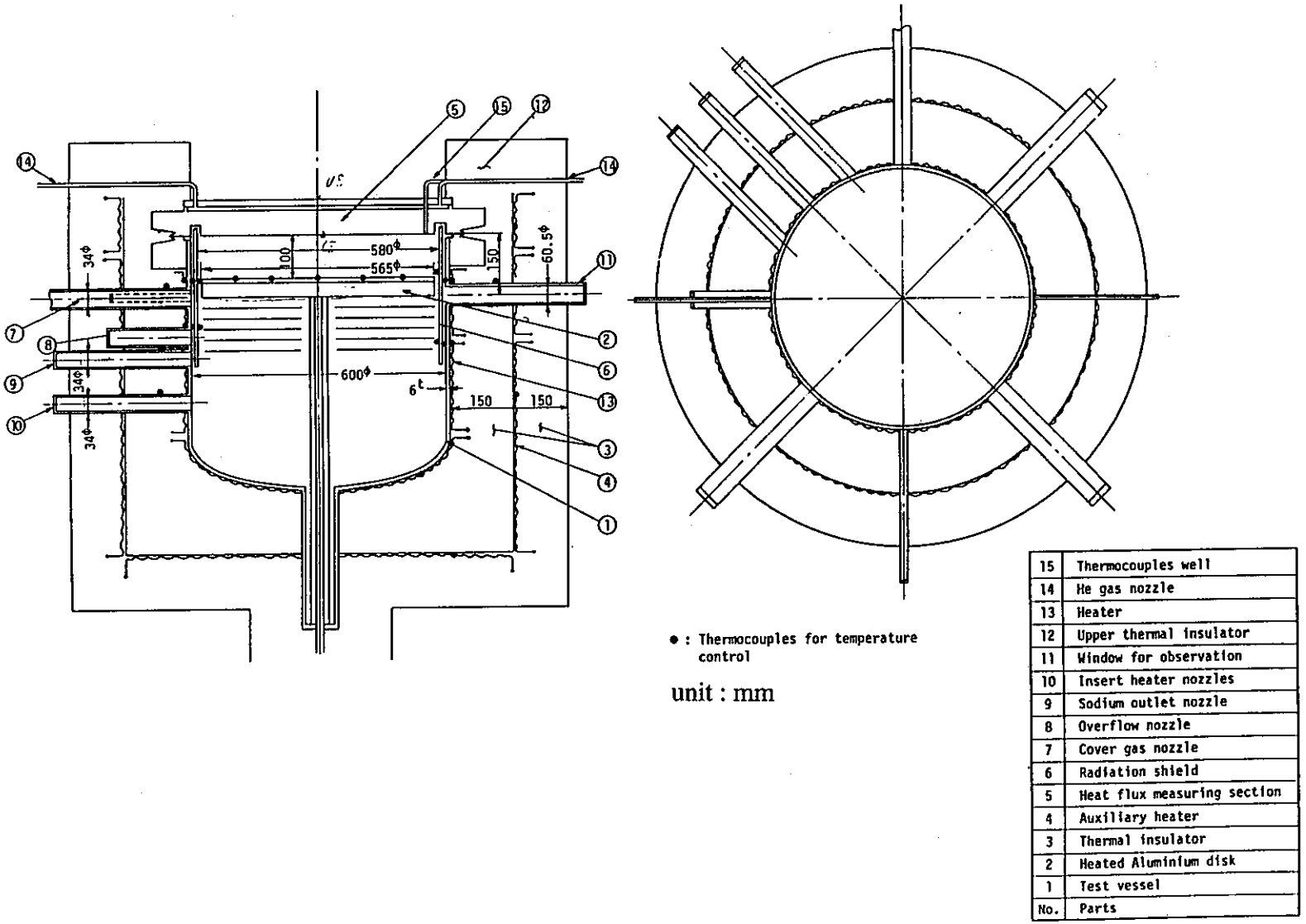

No.	Parts
15	Thermocouples well
14	He gas nozzle
13	Heater
12	Upper thermal insulator
11	Window for observation
10	Insert heater nozzles
9	Sodium outlet nozzle
8	Overflow nozzle
7	Cover gas nozzle
6	Radiation shield
5	Heat flux measuring section
4	Auxiliary heater
3	Thermal insulator
2	Heated Aluminium disk
1	Test vessel

Fig. 2.1 Schematic of Test Vessel

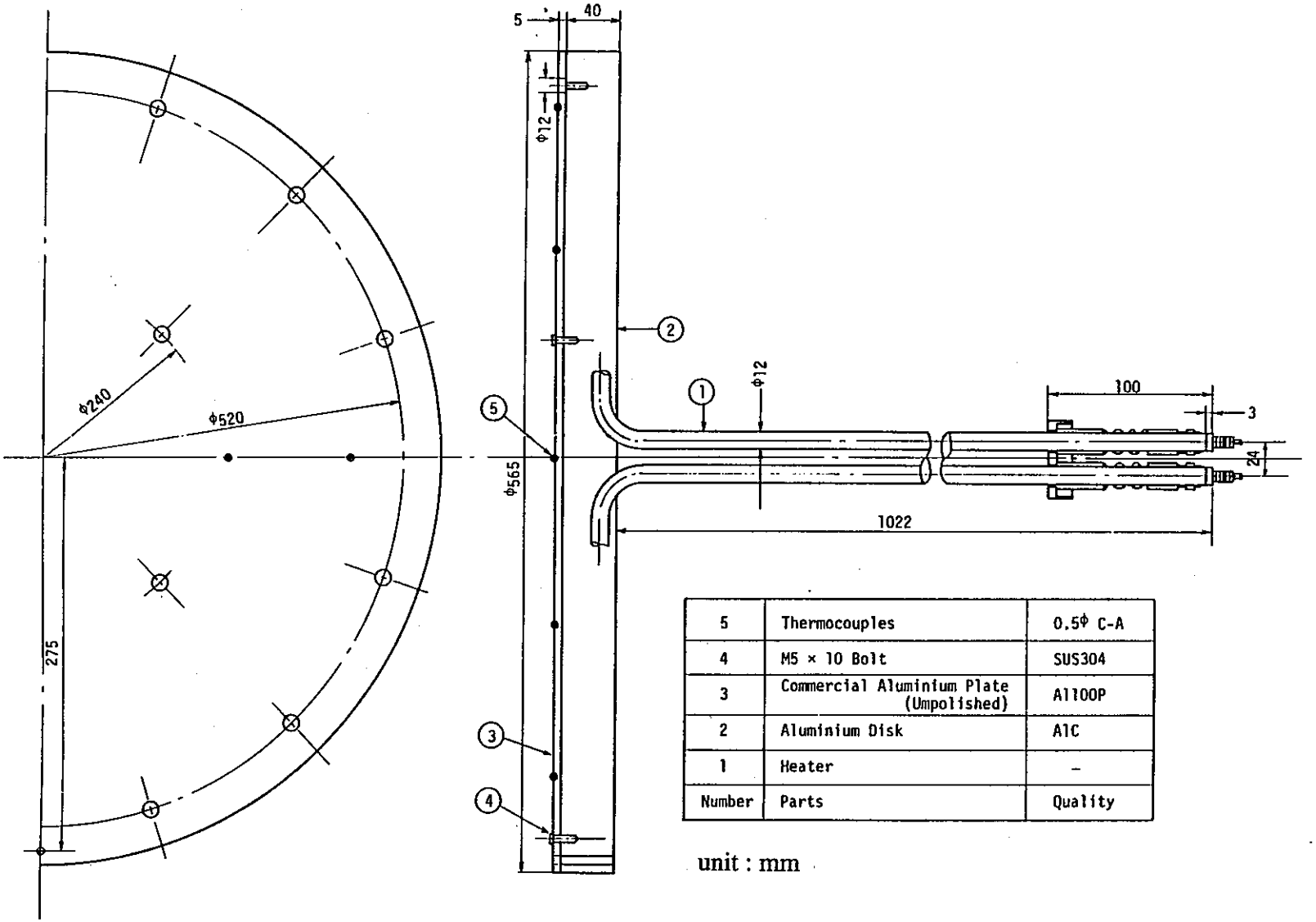

Number	Parts	Quality
5	Thermocouples	0.5φ C-A
4	M5 × 10 Bolt	SUS304
3	Commercial Aluminium Plate (Unpolished)	A1100P
2	Aluminium Disk	A1C
1	Heater	–

Fig. 2.2 Heated Aluminum Disk

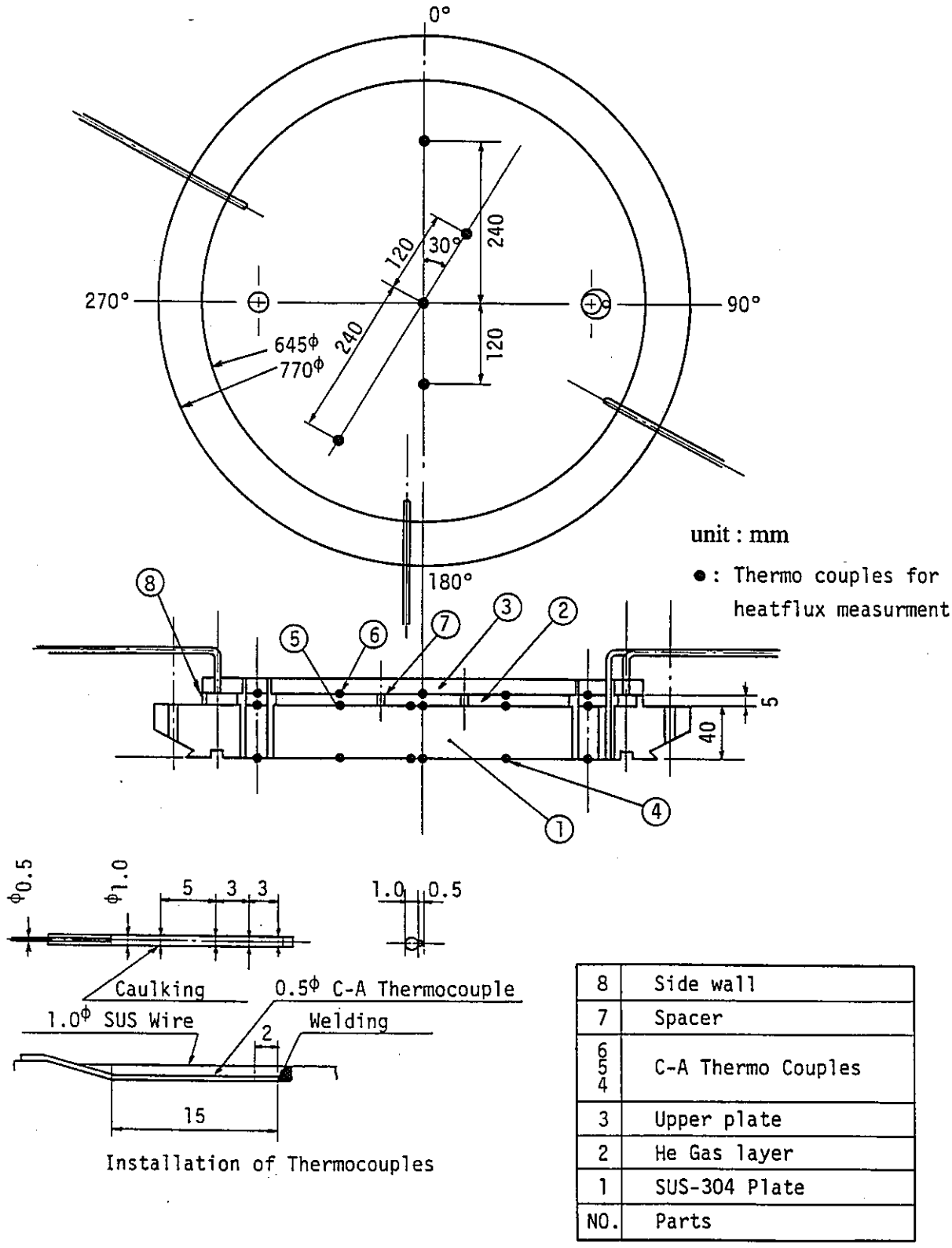

NO.	Parts
8	Side wall
7	Spacer
6 5 4	C-A Thermo Couples
3	Upper plate
2	He Gas layer
1	SUS-304 Plate

Fig. 2.3 Heat Flux Measuring Section

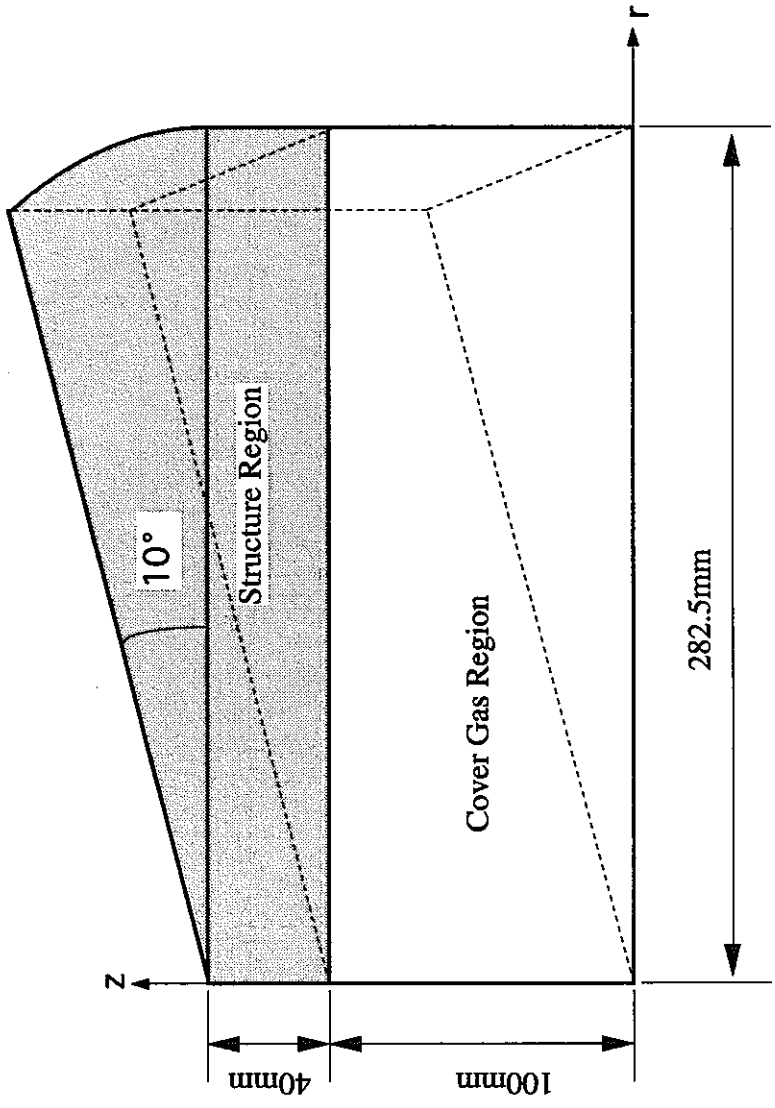

Fig. 4.1 Geometrical Model

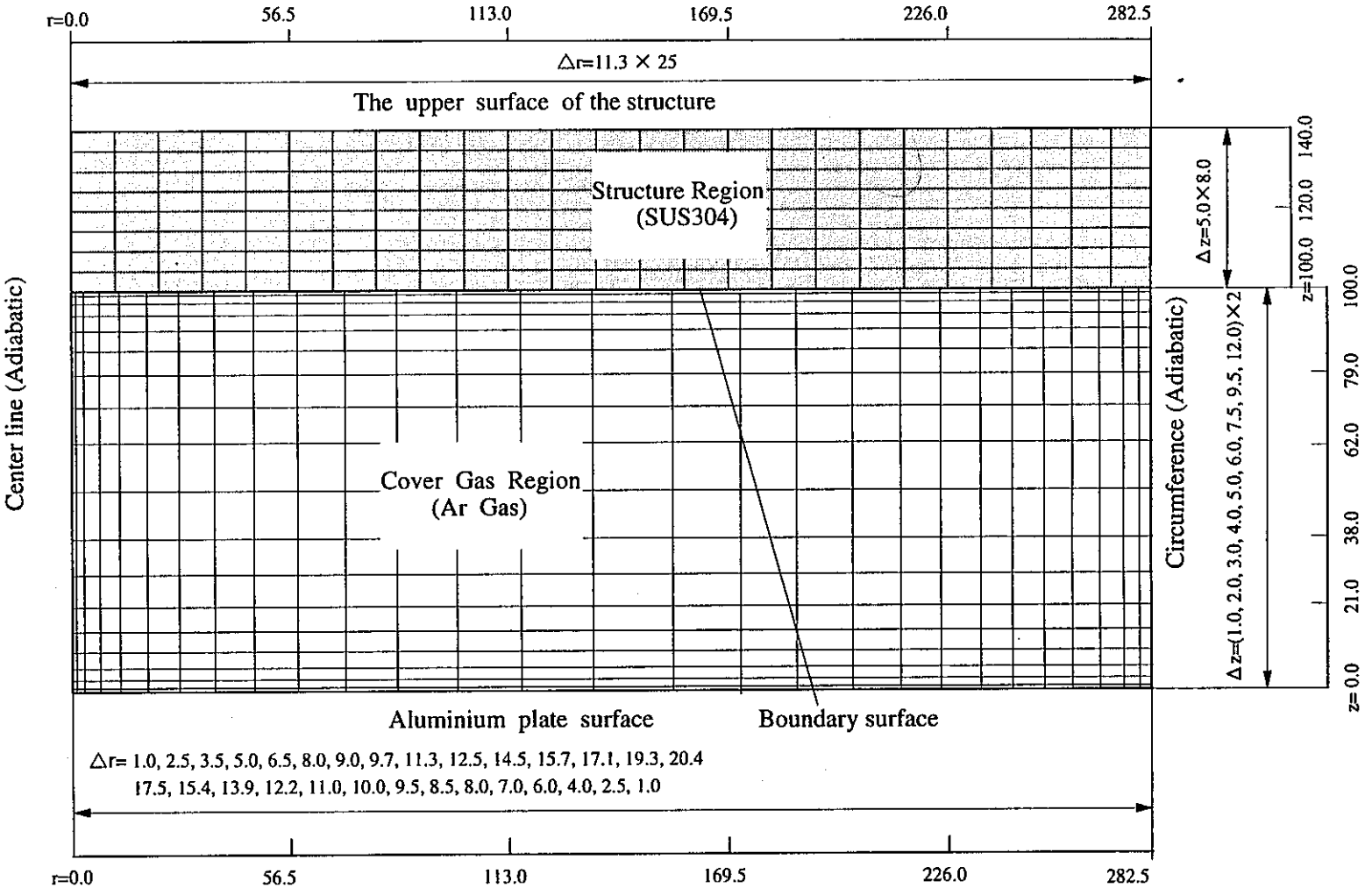

Fig. 4.2 Mesh Arrangement for the Two - Dimensional Calculation

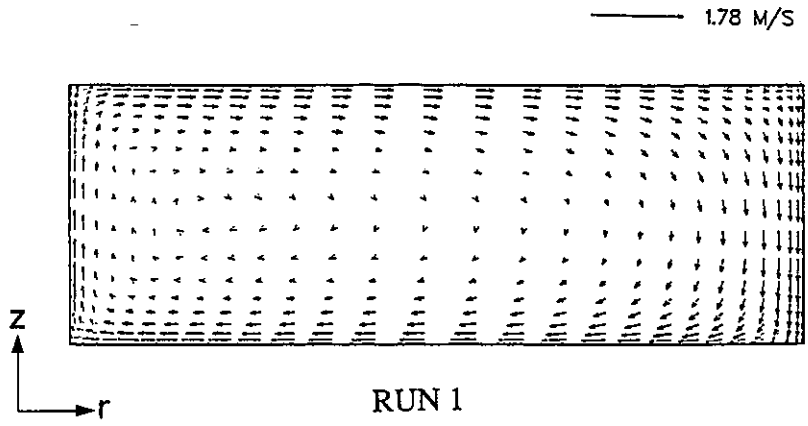

RUN 1

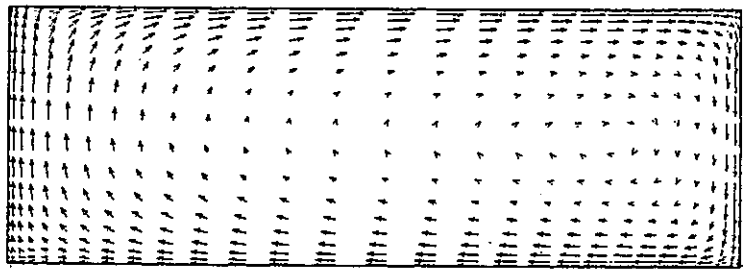

RUN 2

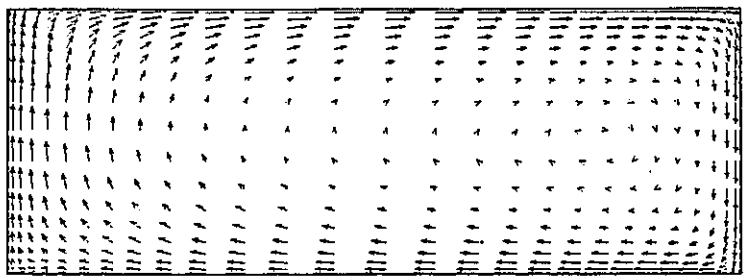

RUN 3

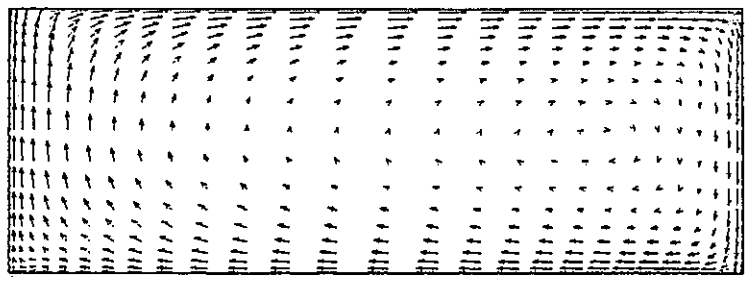

RUN 6

Fig. 5.1.1 Calculated Velocity Vectors in Cover Gas Layer

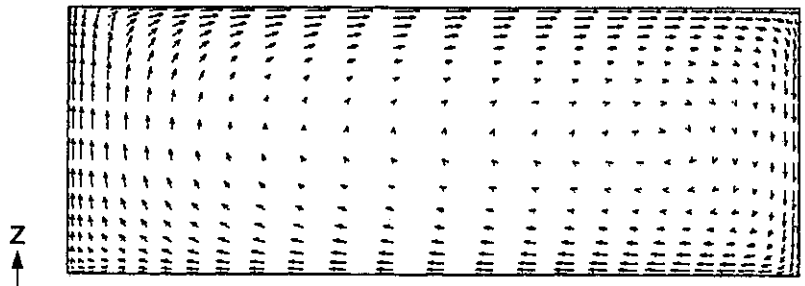

RUN 7

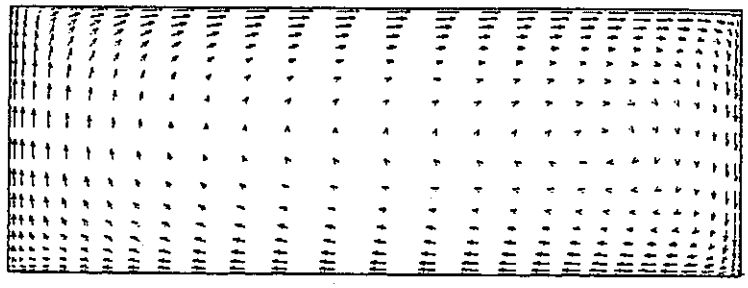

RUN 8

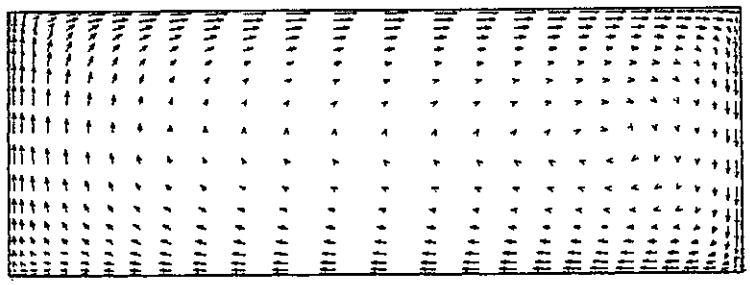

RUN 9

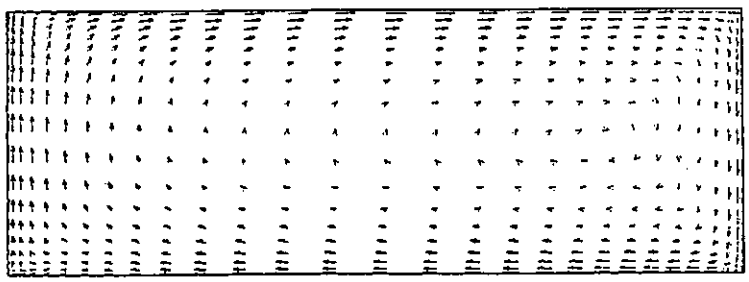

RUN 10

Fig. 5.1.1 Continued

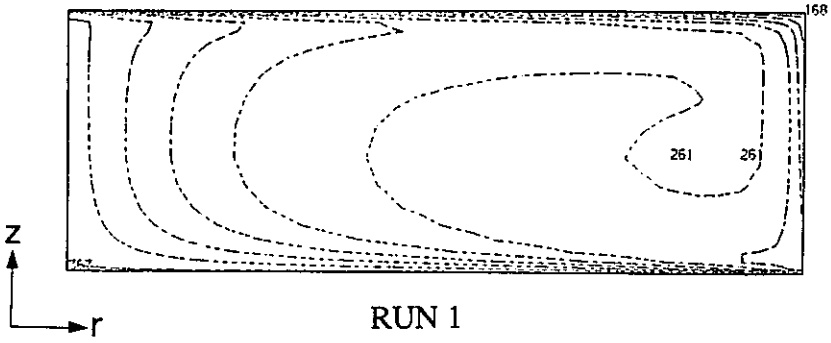

RUN 1

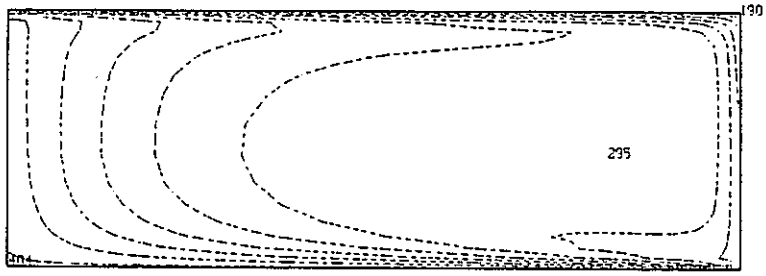

RUN 2

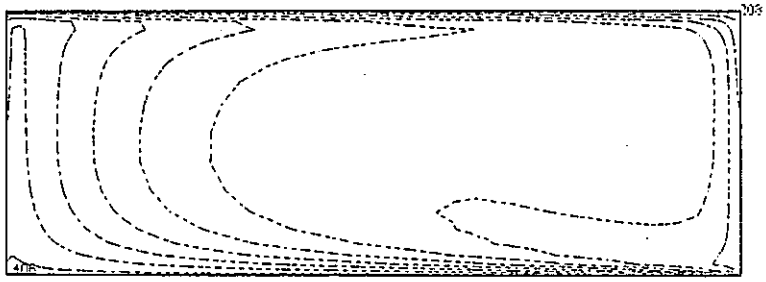

RUN 3

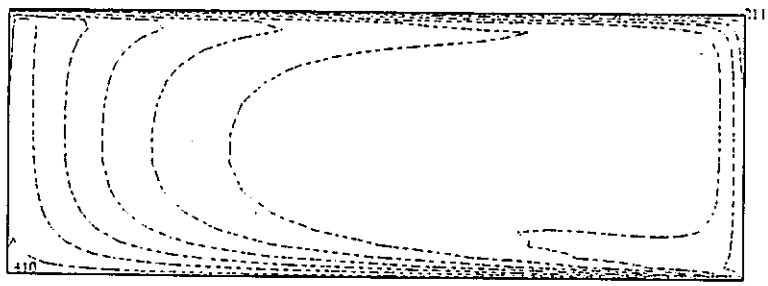

RUN 6

Fig. 5.1.2 Calculated Isotherms in Cover Gas Layer

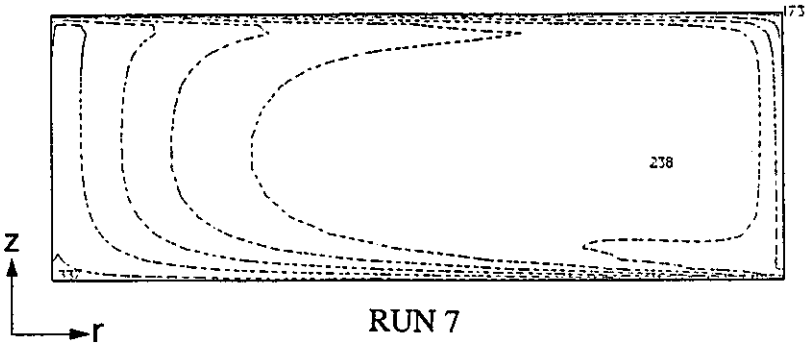

RUN 7

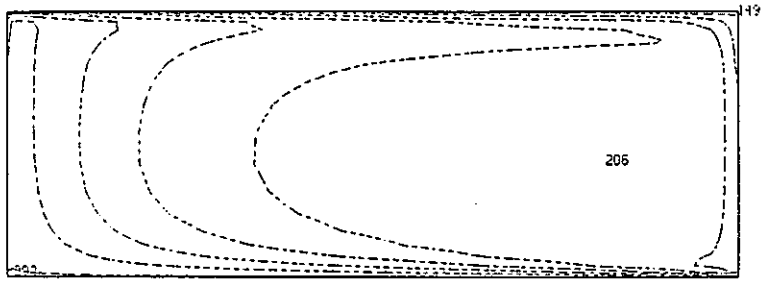

RUN 8

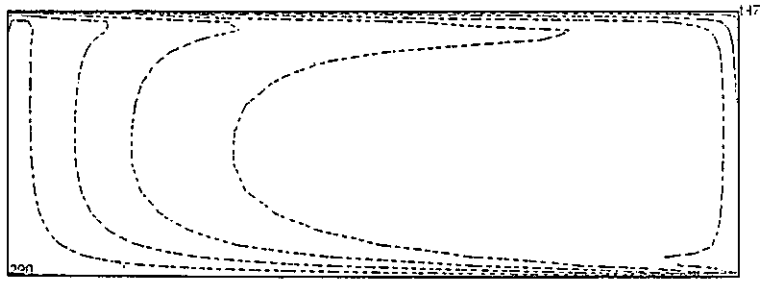

RUN 9

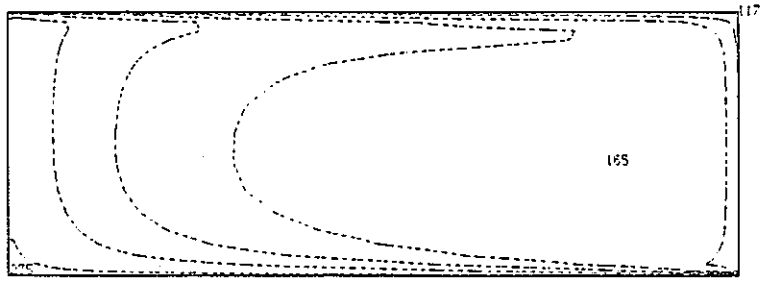

RUN 10

Fig. 5.1.2 Continued

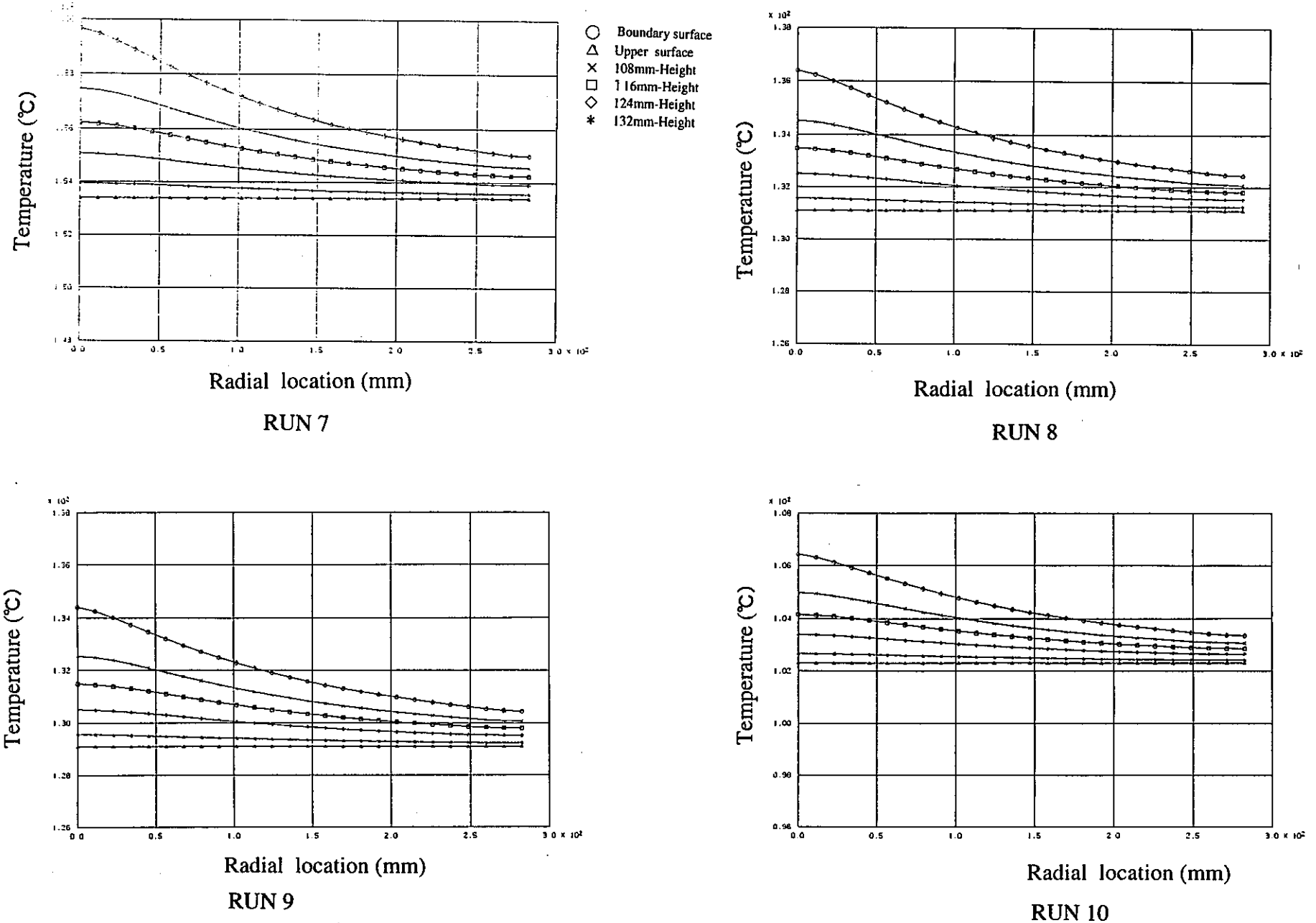

Fig. 5.1.3 Radial Temperature Distributions in Rotating Plug

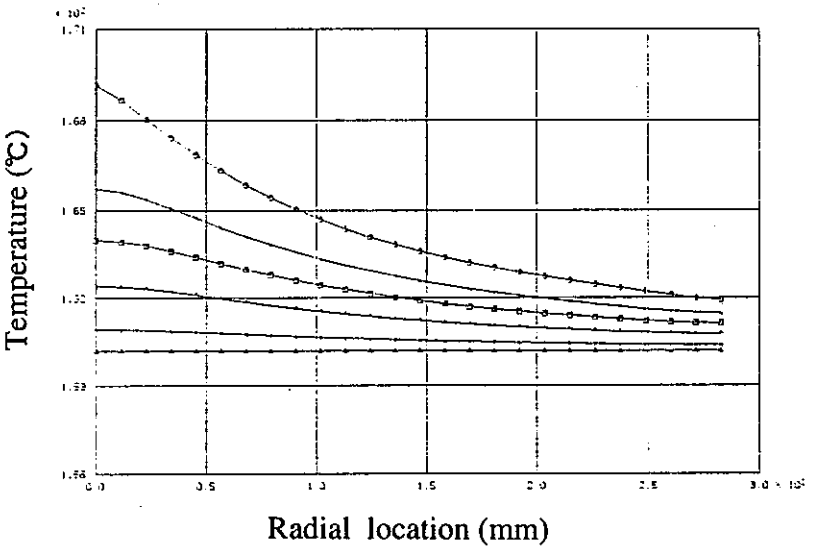

RUN 1

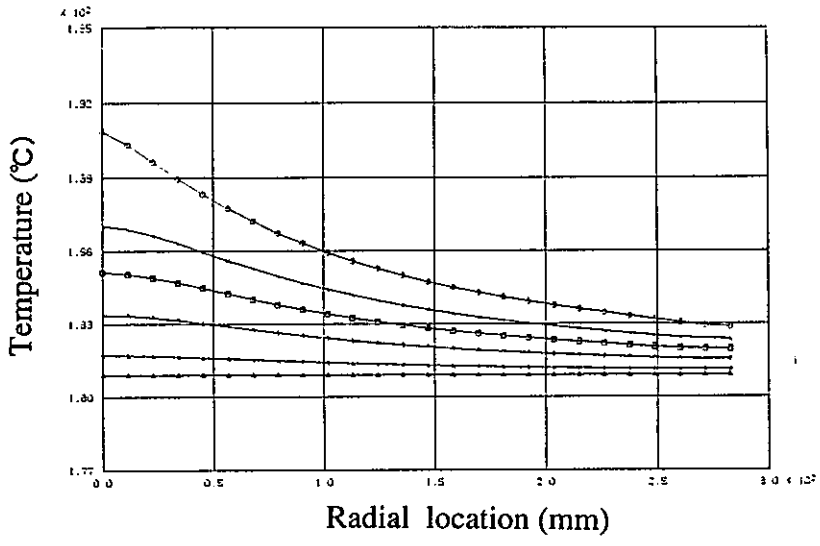

RUN 2

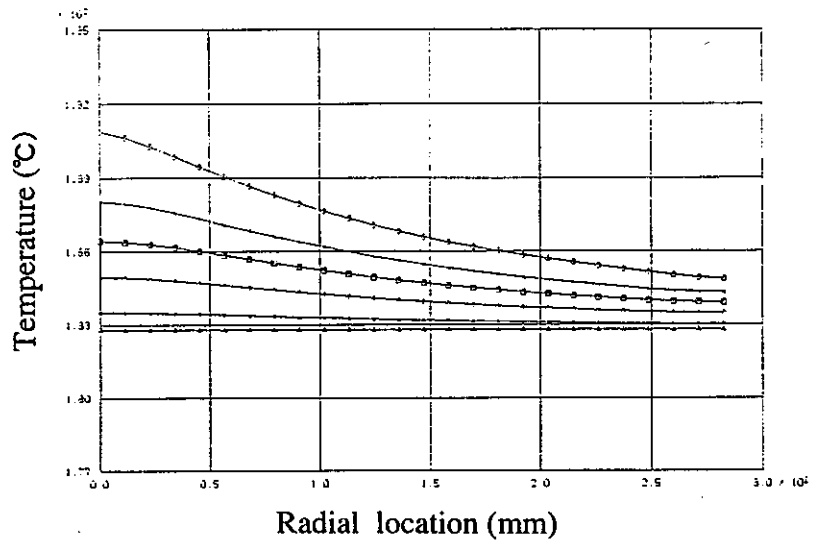

RUN 3

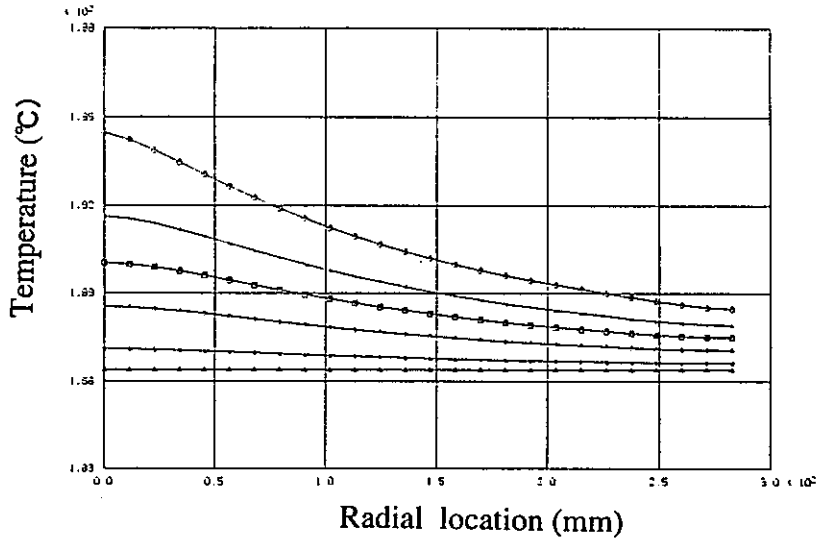

RUN 6

Fig. 5.1.3 Continued

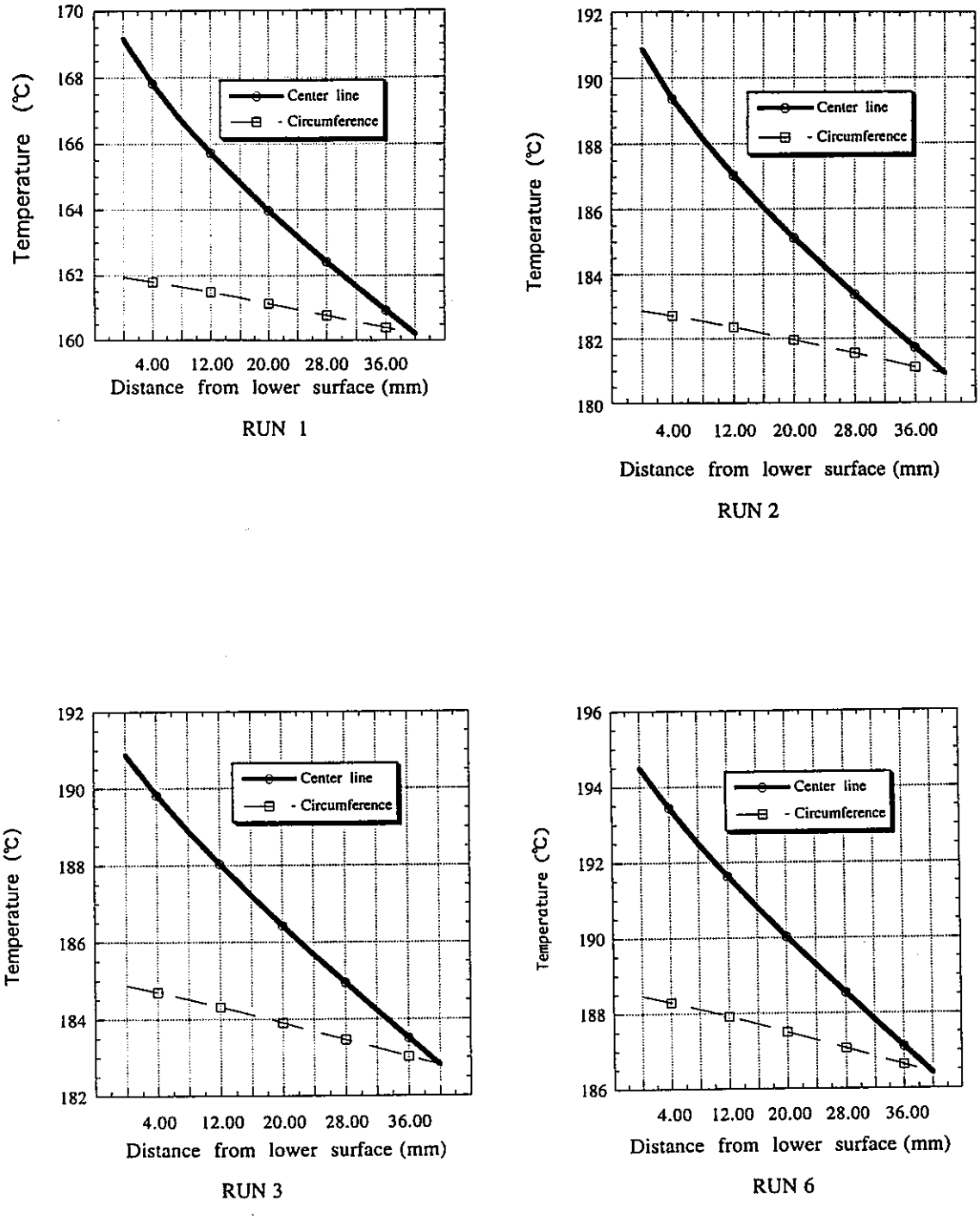

Fig. 5.1.4 Axial Temperature Distribution in Rotating Plug.

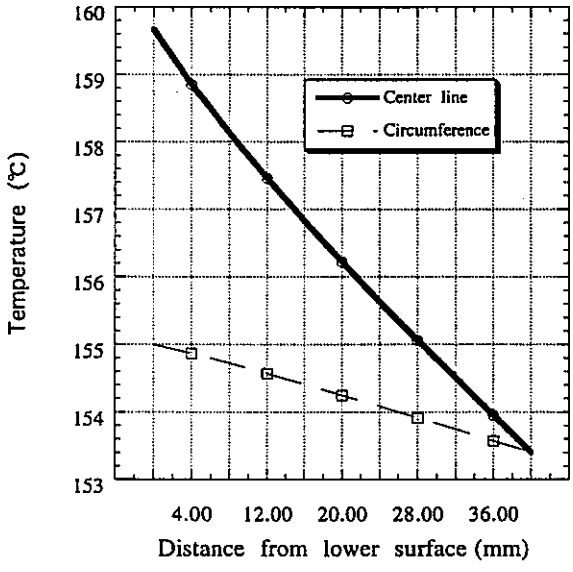

RUN 7

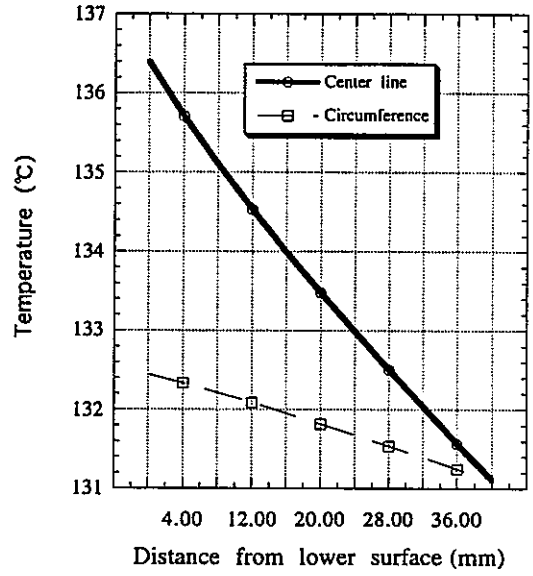

RUN 8

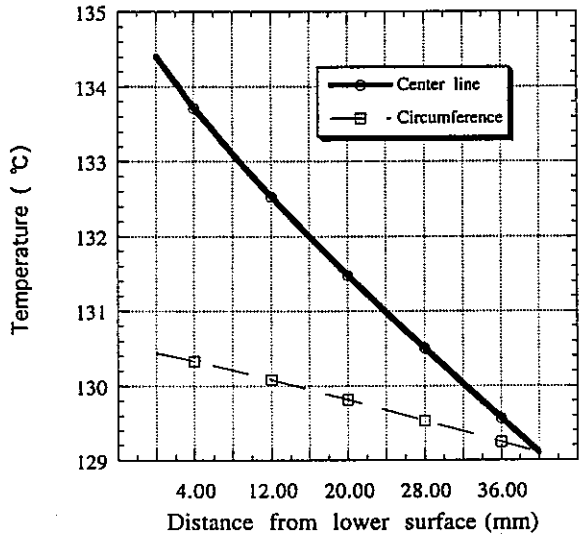

RUN 9

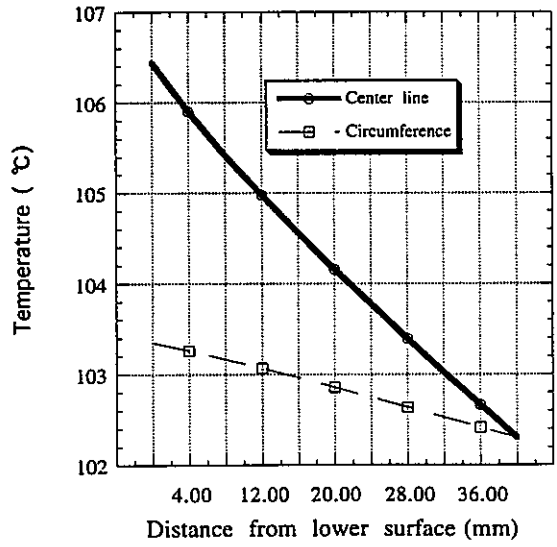

RUN 10

Fig. 5.1.4 Continued.

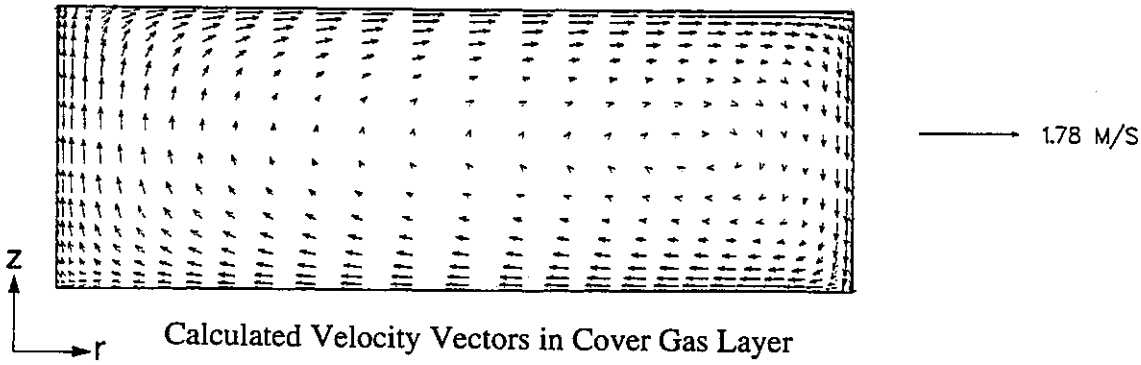

Calculated Velocity Vectors in Cover Gas Layer

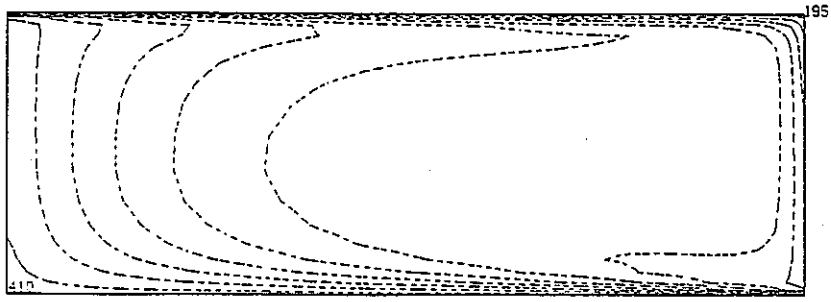

Calculated Isotherms in Cover Gas Layer

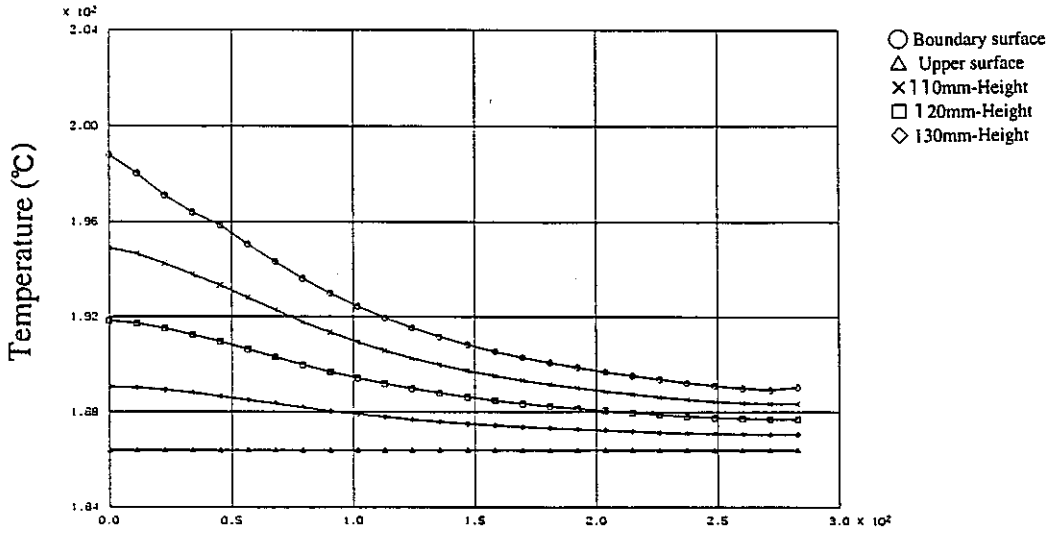

Radial Temperature Distributions in Rotating Plug

Fig. 5.2.1 Calculated Thermal Characteristics for RUN 6
(Considering the Radiant Heat Transfer)

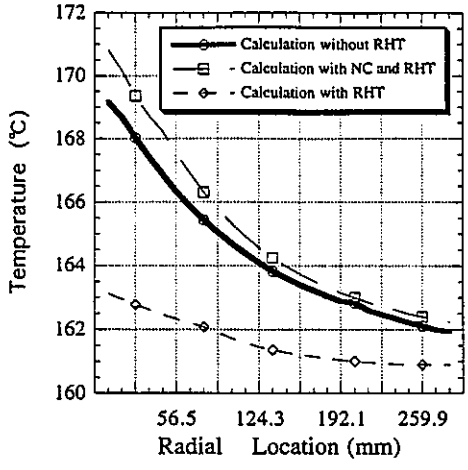

RUN 1

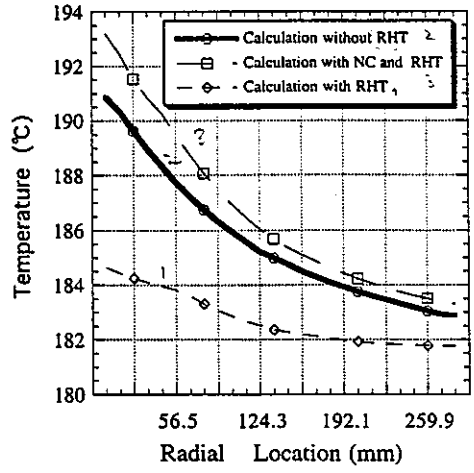

RUN 2

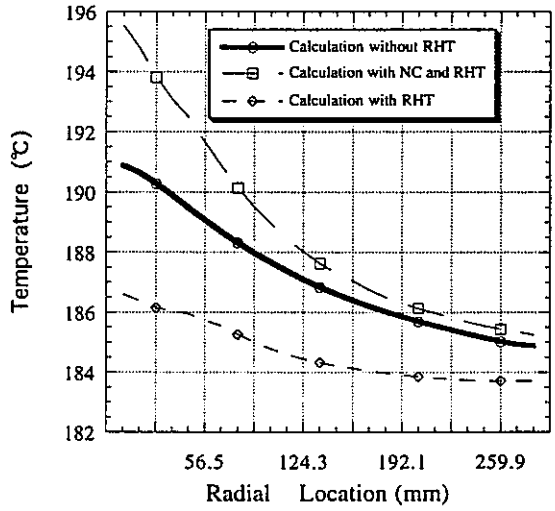

RUN 3

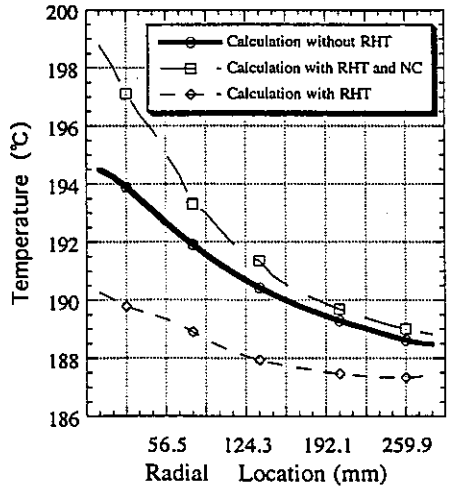

RUN 6

Fig. 5.2.2 Comparison of Boundary Temperature Distributions

APPENDIX

List of FLUSH Input Data for the Two-dimensional Analysis of Experimental RUN1 (with Radiation)

```
SYSTEM
*****************************************************************
**            <<<  RUN 1 INTERFACE ELEMENT  >>>                **
*****************************************************************
STEADY STATE
CYCLE              15          1    1000000       0.01
RESTART    AQUA
CONDITION     3.00E-4    2.40E-5           1
SYSUNIT    2.3883E-10    5.00E-1
******* SURFACE 3 *********
WCELL           1     1    18    29     1    18     3     1
WELEM       100125001 1000
END SYSTEM
*****************************************************************
SAQUA
*****************************************************************
******  COVER-GAS(AR) NATURAL CIRCULATION ANALYSIS      ***********
******             STEADY  RUN EXPERIMENTAL RUN 1        ***********
*****************************************************************
 &GEOM ITURKE=0,
       IFRES=1,  ISYMCH=3, IFITEN=3, IFPCG=5,
       IGEOM=-1, NL1=1138, NM1=522,
       IMAX=29,  JMAX=1,   KMAX=18,  NSURF=6,
       DX= 0.0010, 0.0025, 0.0035, 0.0050, 0.0065, 0.0080, 0.0090,
           0.0097, 0.0113, 0.0125, 0.0145, 0.0157, 0.0171, 0.0193,
           0.0204,
           0.0175, 0.0154, 0.0139, 0.0122, 0.0110, 0.0100, 0.0095,
           0.0085, 0.0080, 0.0070, 0.0060, 0.0040, 0.0025, 0.0010,
       DY= 0.1745329252,
       DZ= 0.0010, 0.0020, 0.0030, 0.0040, 0.0050, 0.0060, 0.0075,
           0.0095, 0.0120,
           0.0120, 0.0095,
           0.0075, 0.0060, 0.0050, 0.0040, 0.0030, 0.0020, 0.0010,
       XNORML= 1.0, -1.0,  0.0,  0.0,  0.0,  0.0,
       YNORML= 0.0,  0.0,  0.0,  0.0,  1.0, -1.0,
       ZNORML= 0.0,  0.0, -1.0,  1.0,  0.0,  0.0,
 &END
REG   -1.        1   1   1   1   1  18   1
REG   -1.       29  29   1   1   1  18   2
REG   -1.        1  29   1   1  18  18   3
REG   -1.        1  29   1   1   1   1   4
REG   -1.        1  29   1   1   1  18   5
REG   -1.        1  29   1   1   1  18   6
END
 &DATA
  ISTATE=0, IFENER=1, IFMMO=2, IFMEN=0,
  IDTIME=1, RDTIME=0.8, LASTIT=250, IT=2*1,
  EPS1=1.0E-6, EPS3=5.0E-5, EPS5=1.0E-5, EPS7=5.0E-5,
  KFLOW=6*-3,      KTEMP=2*400,2*1, 2*400
  TEMP=2*0.0, 161.8, 363.1, 2*0.0,
  TEMP0=265.0, PRES0= 1.6000E+5, GRAVZ=-9.807,
  XPRES0=0.142, YPRES0=0.085,ZPRES0=0.05,
  IFPROP=1, FC0H=1.43216E5,   FC1H=5.21000E2,
            FC0RO=2.338851,   FC1RO=-2.978776E-3,
            FC0K=1.71811E-2,  FC1K=3.94171E-5,
            FC0MU=2.23336E-5, FC1MU=4.90286E-8,
```

```
                FCOCP=521.000,     FC1CP=0.000,
  FCTLO=150.0,FCTHI=650.0,
  NTMAX=100000,      NTPRNT=0,    NTPLOT=0,
  NTHPR=012001,032001,052001,902003,902004,
 &END
END
WL  0.00001       1  29    1    1    1  17
END
END SAQUA
*************************************************************************
SAQUAR
 &GEOM
    IFRES=3,
 &END
 &DATA
    ISTATE=1,TREST=60.0,
    EPS1=5.0E-7,EPS3=1.0E-5,EPS5=5.0E-6,EPS7=1.0E-5
  NTHPR=012001,032001,052001,902003,902004,
 &END
END
END
END SAQUAR
*************************************************************************
SFINAS
FINAS
TITLE       RUN 1 MODEL
HEAT
SAVE
NOPRINT DESCR
CONTROL
    HEAT SOLVE               3
MODEL
COORDINATE SYSTEM
   10    2          0.0        0.0        0.0        1.0        0.0        0.
                    1.0        1.0        0.0
NODE
**NLOOP2       2    1       0.00      10.00       0.00
**NLOOP1       9   10       0.00       0.00       5.00
26001  1001   10              0.00       0.00     100.00              25       1
26001   10              282.50       0.00     100.00
**END1
**END2
  501   10              140.00       5.00       1.00
  601   10              140.00       5.00      99.00
ELEMENT TYPE
   10     HHEX8
   30     RLINK2
CONNECTION
**ELOOP2       8   10   10   10   10   10   10   10   10   10
**ELOOP1      25 1000 1000 1000 1000 1000 1000 1000 1000 1000
 1001   10        100 2002 1002 2001 1001 2012 1012 2011 1011
**END1
**END2
  501   30  400        501  601
GEOMETRY
  400    4 2.500E+05 1.350E-17       0.09      0.018
```

```
FASTENING
  500
     F3      601       0.000E+00    52
            1001       0.100E-02 2001       0.500E-02 3001       0.800E-02
            4001       1.200E-02 5001       1.900E-02 6001       2.000E-02
            7001       2.100E-02 8001       2.100E-02 9001       2.100E-02
           10001       2.100E-0211001       2.100E-0212001       2.100E-02
           13001       2.100E-0214001       2.100E-0215001       2.100E-02
           16001       2.100E-0217001       2.100E-0218001       2.100E-02
           19001       2.100E-0220001       2.200E-0221001       2.200E-02
           22001       2.200E-0223001       2.300E-0224001       2.400E-02
           25001       2.500E-0226001       2.400E-02 1002       0.100E-02
            2002       0.500E-02 3002       0.800E-02 4002       1.200E-02
            5002       1.900E-02 6002       2.000E-02 7002       2.100E-02
            8002       2.100E-02 9002       2.100E-0210002       2.100E-02
           11002       2.100E-0212002       2.100E-0213002       2.100E-02
           14002       2.100E-0215002       2.100E-0216002       2.100E-02
           17002       2.100E-0218002       2.100E-0219002       2.100E-02
           20002       2.200E-0221002       2.200E-0222002       2.200E-02
           23002       2.300E-0224002       2.400E-0225002       2.500E-02
           26002       2.400E-02
MATERIAL
  100    1    SUS304
SPECIFIED TEMPERATURE
  200
           108126081 1000          -39.80
           108226082 1000          -39.80
            501                    163.10
INITIAL TEMPERATURE
            501  601  100          200.00
           100126001 1000          200.00
           101126011 1000          200.00
           102126021 1000          200.00
           103126031 1000          200.00
           104126041 1000          200.00
           105126051 1000          200.00
           106126061 1000          200.00
           107126071 1000          200.00
           108126081 1000          200.00
           100226002 1000          200.00
           101226012 1000          200.00
           102226022 1000          200.00
           103226032 1000          200.00
           104226042 1000          200.00
           105226052 1000          200.00
           106226062 1000          200.00
           107226072 1000          200.00
           108226082 1000          200.00
HEAT INPUT
  500
=READ        21
HISTORY
INTERVAL      1
          SPEC   200   1.0
          HEAT   500   1.0
          FAS    500   1.0
```

```
END MODEL
OUTPUT
PRINT SELECT
TEMP       ALL
ELM        ALL
POST TAPE
TEMP       ALL
ELM        ALL
STRUCTURE PLOT
PESET2          4 100126001 1000 101126011 1000 102126021 1000 103126031 1
                  104126041 1000 105126051 1000 106126061 1000 107126071 1
                  108126081 1000
¥
FRAME       A4V
AXES      -Y     X     Z
VIEW       0.          0.          0.
PTITLE     SAMPLE PLOT
IPLOT          -4      NODES
CPLOT          -4       TEMP      10
¥
END OUTPUT
END FINAS
************************************************************************
FINAS
DUMMY
END FINAS
************************************************************************
FNSEDIT
SELECT TEMP TAPES=1
ST1 ALL
REF TEMP 182.0
END SELECT
END FNSEDIT
```